Time-resolved rheometry *)

M. Mours and H. H. Winter

Department of Chemical Engineering, University of Massachusetts, Amherst, Massachusetts, USA

Abstract: Applicability and limits of time-resolved rheometry have been analyzed for polymers which undergo change during a rheological measurement. Processes such as gelation, phase transition, polymerization or decomposition affect the molecular mobility in these polymers and therefore the rheological experiment. We propose to choose the well known effect of heating (or cooling) during the relaxation and analyze it as a paradigm for rheometry on samples with changing molecular mobility. The temperature change does not cause permanent changes in sample structure, but it affects the molecular mobility and it significantly interferes with the measurement if the temperature changes occur too fast. In this study, time-resolved mechanical spectroscopy (TRMS) was used to experimentally investigate the effect of heating on the relaxation behavior of a typical polycarbonate sample. Each data point in a cyclic frequency sweep (CFS) was taken at a different state of the material; the data were interpolated using an interactive computer program. In this fashion, a single TRMS experiment yielded a master curve over eight decades. A model for relaxation under non-isothermal conditions showed the limitations of TRMS. It could be demonstrated that TRMS worked well for sufficiently small mutation numbers, i.e., for sufficiently small changes during the measurement. A critical mutation number of 0.9 was determined for the non-isothermal case beyond which the material response became non-linear. This corresponds to a calculated relative change of the shear stress amplitude of about 90%.

Key words: Time-resolved mechanical spectroscopy − relaxation − non-isothermal flow − mutation number

Introduction

A stable sample is usually considered as prerequisite for a meaningful rheological measurement. This excludes materials with changing structure such as polymers during gelation, phase transition, decomposition, polymerization, etc., but since these materials have very distinct properties, their investigation and utilization has become more and more common in recent years. A time-resolved rheometry (TRR) technique is needed which enables characterization of the dynamic properties of such transient polymers.

In the following, we will use the term "mutation" as a general expression for changes of either molecular weight, molecular weight distribution, connectivity between molecules, aggregation, ordering on super-molecular scale (by phase separation in a polymer blend or block-copolymer, for instance), or other structural phenomena which affect molecular mobility. Very different types of structural changes can have similar influences on the rheological behavior. For crosslinking materials, the structural evolution depends on the extent of reaction p which is equal to the number of actual chemical bonds divided by the maximum possible number of bonds. We will borrow symbol p to identify the structural state of a changing material without specifying the type of structural change.

The linear viscoelastic behavior of a transient material may be expressed as

$$\tau = \int_{-\infty \ t''=t'}^{t \quad t''=t} G\ (t,t',p(t''))2D(t')dt' \ , \tag{1}$$

where τ is the stress tensor and D is the rate of strain

---

*) Dedicated to Prof. Ken Walters on the occasion of his 60th birthday.

tensor. The relaxation functional $\underset{t''=t'}{\overset{t''=t}{G}}$ $(t,t',p(t''))$ is positive valued. It has to account for mutation during the relaxation processes. In most cases, $\underset{t''=t'}{\overset{t''=t}{G}}$ $(t,t',p(t''))$ decays monotonously with $(t-t')$, but it cannot be excluded that $\underset{t''=t'}{\overset{t''=t}{G}}$ $(t,t',p(t''))$ increases due to a change in structural state. $p(t'')$ denotes the changing structural state of the material at intermediate times $t'<t''<t$. The equation is based on the linear superposition principle of stress and strain. Its range of validity is restricted to sufficiently small strains.

In the case of a stable sample, the above equation reduces to the classical Boltzmann equation (e.g., Ferry, 1980)

$$\tau = \int_{-\infty}^{t} G(t-t')2D(t')dt' \ . \tag{2}$$

The relaxation modulus $G(t-t')$ often is represented as Laplace Transform of the relaxation time spectrum $H(\lambda)$

$$G(t-t') = \int_{0}^{\infty} H(\lambda)e^{-(t-t')/\lambda}\frac{d\lambda}{\lambda} \ . \tag{3}$$

For time-resolved rheometry, one would like to describe each of the structural states p with its own relaxation modulus $G(t-t')$ or its own spectrum $H(\lambda)$.

An ideal way of quantifying the rheology at evolving structural states p would be to stop the ongoing sample mutation (crosslinking, phase transition, etc.) at intermediate states and measure G or H on the stable samples. For crosslinking polymers, this has been possible by catalyst poisoning (Chambon et al., 1985) and has resulted in much insight in the rheological changes near liquid solid transition. However, stopping of the mutation process is possible only in exceptional cases.

The rate of mutation is small in some materials so that intermediate states $p(t'')$ can be treated as constant during the taking of individual data points. The relaxation functional reduces to $G(t-t', p_0)$ for these materials which we will call "quasi-stable".

For materials with rapidly changing material structure, $\underset{t''=t'}{\overset{t''=t}{G}}$ $(t,t',p(t''))$ cannot be reduced in general.

Stress calculation requires a constitutive model which accommodates the structural changes during relaxation. Very little is known about such structural constitutive models so that it is difficult to estimate the cross-over from a quasi-stable to an unstable sample.

Characteristic time scales of rheometry

Characterization techniques for determining dynamic properties, such as time constants and relaxation rates of viscoelastic materials, genuinely differ from the techniques for static properties. Static properties are not constrained by any material inherent time constants and the experimental time (time required by the measuring apparatus to obtain the value of the desired static property) depends on the configuration of the experiment only, i.e., it does not depend on the characteristics of the investigated material. This can be exemplified with time-resolved small-angle x-ray measurements (SAXS) or transient temperature measurements: SAXS measurements can be accelerated by increasing the scattering contrast or the beam intensity; transient temperature measurements can be made nearly instantaneously due to the short response time of temperature probes.

Contrary to these static property measurements, experimental times for determining dynamic properties depend on the sample-inherent time behavior, e.g., the duration of a rheological experiment is dictated by the molecular mobility of the sample. Even if stress and strain can be measured instantaneously (within nanoseconds), the measurement has to last over a time period in which the material structure can respond to an imposed strain or stress. This inherently prevents shortening of the experimental time below the material-imposed time limit and, consequently, sample stability or quasi-stability is necessary for a meaningful rheological measurement. Three time constants govern time-resolved rheometry:

1) the material time λ is the time constant of the relaxation mode which dominates the rheometrical experiment;

2) the duration of the rheological experiment defines the experimental time Δt. A dynamic mechanical experiment, for instance, requires measurement times in order of the relaxation mode which one wants to probe, and measurement of steady-state properties requires waiting until steady state is reached (in the order of the longest mode);

3) the mutation time λ_{mu} is the characteristic time constant for the change in the material

$$\lambda_{\mathrm{mu}} = \left[\frac{1}{g} \frac{\partial g}{\partial t} \right]^{-1} . \tag{4}$$

The change is not measured directly, but rather indirectly through the property of interest, g, which has to be specified for each type of experiment. λ_{mu} is defined as the time which is required for a $(1/e)$-change of property g at the instantaneous rate of change $\partial g/\partial t$.

The three time constants combine naturally into two dimensionless groups: the first one is the Deborah number (Reiner, 1964)

$$N_{\mathrm{De}} = \lambda/\Delta t , \tag{5}$$

which compares the material time to the experimental time. Its value decides the importance of viscoelasticity in an experiment. The second dimensionless group is the mutation number (Winter et al., 1988)

$$N_{\mathrm{mu}} = \Delta t/\lambda_{\mathrm{mu}} \tag{6}$$

which estimates the change during an experiment. For small N_{mu}, the mutation is small enough to be negligible in the analysis of an experiment. With the above two dimensionless groups, one can form a third one,

$$N_{\mathrm{De}} N_{\mathrm{mu}} = \lambda/\lambda_{\mathrm{mu}} \tag{7}$$

which compares the material time to the time of material change. This group is equally instructive, since it immediately decides on the feasibility of an experiment. The characteristic time λ can be measured directly and the sample can be treated as quasi-stable if $\lambda/\lambda_{\mathrm{mu}} \ll 1$, while a detailed model (relaxation functional) of the changing sample is required if $\lambda/\lambda_{\mathrm{mu}} \geq 1$ since the sample changes during the relaxation process. This problem will be addressed throughout the paper.

It should be stressed that the following arguments are not restricted to rheometry. The same time constraints as described here for time-resolved rheometry apply to well-known time-resolved dielectric measurements as well (g would be defined by dielectric properties ε' or ε'', for instance) and to the measurement of dynamic properties in general.

Time-resolved mechanical spectroscopy

We will investigate the transient samples specifically in dynamic mechanical experiments. The samples will be probed by an imposed small amplitude oscillatory strain (amplitude γ_0, frequency ω). Properties of interest are the dynamic moduli, G' and G'', which are related to the shear stress response (amplitude τ_0, frequency ω, phase angle δ) by

$$G' = \frac{\tau_0}{\gamma_0} \cos (\delta) \tag{8}$$

$$G'' = \frac{\tau_0}{\gamma_0} \sin (\delta) . \tag{9}$$

The time constants of such "time-resolved mechanical spectroscopy" (TRMS) are easily defined: The experimental time Δt is the duration of a single measurement, i.e., the time required by the rheometer to take a data point. For TRMS it is approximately given by the period of the oscillatory shear

$$\Delta t \cong 2\pi/\omega . \tag{10}$$

During this period the shear stress response is measured continuously and then transformed into a single data point for each, G' and G'', by use of Eqs. (8) and (9), respectively. Δt can be preceded by another time period Δt_w during which the material reaches a quasi steady state. No measurement is taken during Δt_w.

Mechanical spectroscopy predominantly probes the relaxation modes near $\lambda = 1/\omega$ (see Appendix) so that the Deborah number reduces to

$$N_{\mathrm{De}} \cong \lambda \omega/2\pi = 1/2\pi . \tag{11}$$

The mutation time refers to the properties $g = G'$ and $g = G''$:

$$\lambda'_{\mathrm{mu}} = \left[\frac{1}{G'} \frac{\partial G'}{\partial t} \right]^{-1} \quad \text{and} \quad \lambda''_{\mathrm{mu}} = \left[\frac{1}{G''} \frac{\partial G''}{\partial t} \right]^{-1} . \tag{12a,b}$$

The mutation number has to be evaluated for both G' and G'':

$$N'_{\mathrm{mu}} = \frac{2\pi}{\omega G'} \frac{\partial G'}{\partial t} \quad \text{and} \quad N''_{\mathrm{mu}} = \frac{2\pi}{\omega G''} \frac{\partial G''}{\partial t} , \tag{13a,b}$$

and the larger value determines the limits of the experiment (usually, G' responds more sensitively for transient materials). The two dimensionless groups may be combined into

$$N_{De}N'_{mu} = \frac{\lambda}{G'}\frac{\partial G'}{\partial t} \quad \text{and} \quad N_{De}N''_{mu} = \frac{\lambda}{G''}\frac{\partial G''}{\partial t} .$$

$$(14a,b)$$

Dynamic mechanical experiments become non-linear when N_{mu} or $N_{De}N_{mu}$ exceed certain values which have to be quantified for each mutation process. Winter et al. (1988) found, for instance, that in a gelation experiment non-linear effects were negligible for N_{mu} smaller than 0.15. Below this critical value, the sample can be assumed to be quasi-stable during the experimental time.

The characterization of a quasi-stable sample can be understood by looking at the schematic plot in Fig. 1. The material property g changes during the entire experiment. If the probing time or the rate of overall property change is small, the sample behaves quasi-stable during the experimental time Δt (e.g., sinusoidal stress response to an imposed sinusoidal strain). In this case, each measured value of property g (e.g., G', G'') represents a distinct (quasi-stable) state of the material.

TRMS in its most simple form would probe the material at a *single* frequency and record the changing G', G'', $\tan\delta$, etc. with time. This is a standard feature of commercial rheometers and many researchers use it as a well established characterization method. Holly et al. (1988) extended this procedure by probing the material simultaneously with several frequencies. This so-called "multi wave method", "multi frequency method", or "Fourier transform mechanical spectroscopy" has been adopted by several manufacturers of commercial rheometers. It is especially effective when superposing all the lowest frequencies at once.

Scanlan et al. (1991) developed a TRMS method in which they subjected mutating samples to a sequence

of frequencies. They repeated this sequence cyclicly and recorded frequency and time-dependent $G'(\omega,t)$ and $G''(\omega,t)$. Each data point characterized a new state of the material. Data analysis required interpolation procedures, however, applicability and limits were never addressed and studied in depth.

In this study, we will analyze the inherent features and limitations of TRMS by measuring and modeling the special case of thermally induced changes in polymeric materials. Even if thermally induced changes in molecular mobility can not be considered as a mutation in its above definition, their effect on the rheometry is the same in many respects. We propose to use rheometry on samples with thermally induced changes of molecular mobility as a paradigm for rheometry on mutating samples. Instead of p, we use temperature T as state variable.

Thermally induced changes are special in the sense that a physically meaningful model for $\underset{t''=t'}{\overset{t''=t}{G}}$ $(t,t',p(t''))$ has been proposed by Hopkins (1957) and Morland and Lee (1960), resulting in a relaxation modulus which can be written as

$$G(t,t',a_T,b_T)$$
$$= \int_0^\infty b_T H(\lambda) \exp\left(-\frac{1}{\lambda}\int_{t'}^t \frac{dt''}{a_T(t'')}\right)\frac{d\lambda}{\lambda} , \qquad (15)$$

with the temperature shift factors $a_T(t'')$ and b_T. The material change in this case results only in a shift of relaxation times λ_i, but does not affect the shape of the relaxation spectrum itself. Nevertheless, this model can be used to evaluate the effect of changing molecular mobility on dynamic mechanical measurements. Critical values of N_{mu} and $N_{De}N_{mu}$ (corresponding to critical heating rates) can be calculated for the crossover from quasi-stable to unstable material behavior. The predictions will be compared to experiments.

Fig. 1. Material behavior on different time scales (overall experiment, probing time (experimental time Δt), noise)

Experimental

Material

A partially crosslinked polycarbonate, PC Lot 150 as supplied by GE Plastics, was chosen because of its high temperature sensitivity. PC Lot 150 is an isotropic and amorphous polymer. Vitrification occurs at temperatures between 130° and 150 °C, thermal degradation at about 500 °C. The granular material was dried in a vacuum oven at 100 °C for about 24 h.
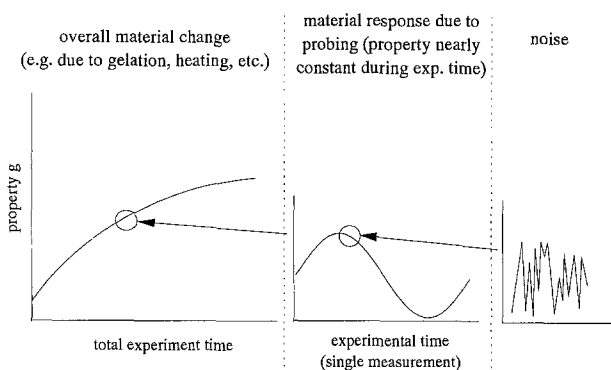
Afterwards, samples were formed using a high-pressure compression molding device. Storage under vacuum prevented rehumidification.

Rheological measurements

For measuring the storage and loss moduli, G' and G'', respectively, as a function of time and frequency, we used a Rheometrics Mechanical Spectrometer, RMS 800, with parallel plate geometry and gap settings of about 1.3 mm. Cyclic frequency sweeps (CFS) gave the time-resolved data. The frequency window $\omega = 0.1 - 100$ rad/s was scanned repeatedly (3 data points per decade) while increasing the temperature linearly from 166° to 280 °C with a heating rate of 1 K/min using an external temperature control. The experimental times Δt for each frequency are prescribed by the Rheometrics instrument. They are approximately given by Eq. (10).

Special attention was given to the heating rate dependence of the data. The material was additionally probed at each of the constant frequencies ($\omega = 0.03$, 0.05, 0.1, and 1 rad/s) with constant heating rates between 0 K/min and 15 K/min. The limiting case of 0 K/min denotes conditions allowing the material to reach steady state at every probed temperature before performing the measurement. Thermal inertia at high heating rates might cause additional problems for our measurement. Such effects will be discussed later in this paper.

Method of data analysis

Due to the rising temperature, the molecular mobility increases and shifts the relaxation time spectrum during the measurement. Each TRMS data point represents a different state of the material and interpolation is necessary to obtain data as a function of frequency at discrete states (i.e., at discrete T-values) of the material (Fig. 2). The interpolation requires a sequence of procedures which has been assigned to a personal computer:

1. Sorting: The data points $G'(\omega_j, T(t))$ and $G''(\omega_j, T(t))$ ($j = 1, 2, \ldots M$, where M is the number of discrete frequencies in the CFS-experiment), initially sorted in terms of increasing time, must be rearranged in terms of increasing frequency.

2. Smoothing: Continuous curves $f_j'(T)$ and $f_j''(T)$ were calculated for each frequency ω_j, representing the evolving moduli $G'(\omega_j, T(t))$ and $G''(\omega_j, T(t))$ as a function of increasing temperature. Data smoothing
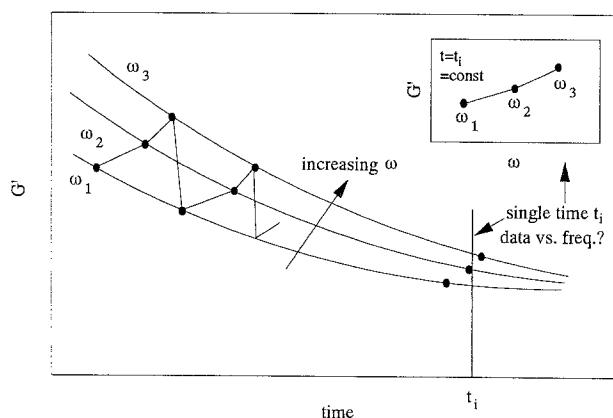

Fig. 2. Schematic plot of results from cyclic frequency sweeps. The symbols in the main plot denote actual data points. Although the measurement for one data point extends over several seconds, a specific time is assigned to each data point by the rheometer control software (no details are given about the criteria for assigning this time). Data vs. frequency (small plot) cannot be determined from measured data points only. Interpolation at times t_i become necessary

in conjunction with the curve fitting gave the most consistent results. The so-called "Cross-Validation-Method" allowed for a good smoothing without any parameter pre-selection (Reinsch, 1967; de Boor, 1978; Craven et al., 1979; Wahba, 1990). This must be repeated for each discrete frequency of the G'- and G''-data set.

3. Interpolation: Using these fitted curves, dynamic mechanical data G', G'', $\tan \delta$, $2\delta/\pi$, etc. can be calculated at discrete temperatures (times) for each of the frequencies. For samples with mutating structure, this set of data $G'(\omega)$, $G''(\omega)$ at discrete states would institute the desired result. However, here we will measure temperature effects and can further advance the analysis through time-temperature superposition.

4. Master curve and spectrum calculation: Time-temperature shifting reduces these interpolated data into a single master curve. Transformation from the frequency to the time domain, using the algorithm of Baumgärtel et al. (1989), resulted in a discrete relaxation time spectrum,

$$H(\lambda) = \sum_{i=1}^{N} g_i \delta(1 - \lambda/\lambda_i) , \tag{16}$$

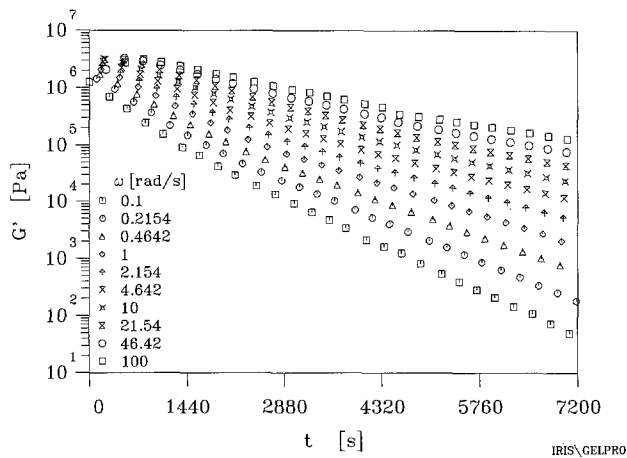which is equivalent to a discrete relaxation modulus (Ferry, 1980):

Fig. 3. Storage moduli $G'(t)$ of polycarbonate at different frequencies ($\omega = 0.1 - 100$ rad/s) and increasing temperature (166° − 280 °C, heating rate 1 K/min) during the CFS-experiment

$$G(t) = \sum_{i=1}^{N} g_i e^{-t/\lambda_i} \ . \tag{17}$$

It consists of a linear superposition of N Maxwell modes of strength g_i and relaxation time λ_i. $\delta(x)$ in Eq. (16) denotes the Dirac delta function.

Experimental results

The data analysis is most easily demonstrated with a specific data set. Figure 3 shows the measured G'-data (cyclic frequency sweeps at linearly increasing temperature). An equivalent G''-data set exists, but is
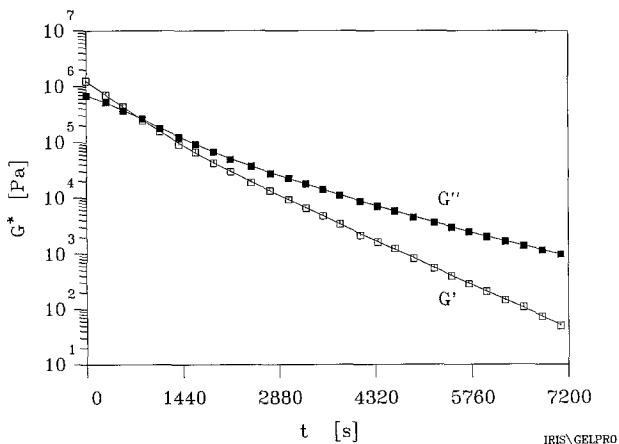

Fig. 4. Storage moduli $G'(t)$ and loss moduli $G''(t)$ of polycarbonate after data rearranging and smoothing ($\omega = 0.1$ rad/s). The symbols represent the actual data points, and the lines represent the smooth curves
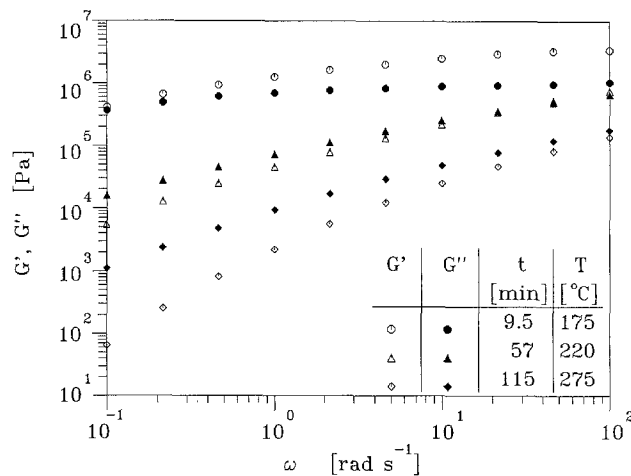

Fig. 5. Calculated storage moduli $G'(\omega)$ and loss moduli $G''(\omega)$ of polycarbonate at different times (i.e., different temperatures, material states)

not shown here. This demonstrates the abundance of data and, therefore, the necessity of a computerized data analysis. A specific time is assigned to each data point by the rheometer control software although each data point measurement extends over several seconds (no details are known about how these times are assigned). After sorting the data points in terms of frequency and data fitting by smooth curves, plots of single frequency data are possible (Fig. 4). Figure 5 shows interpolated data vs. frequency at several discrete temperatures (175°, 220°, and 275 °C).
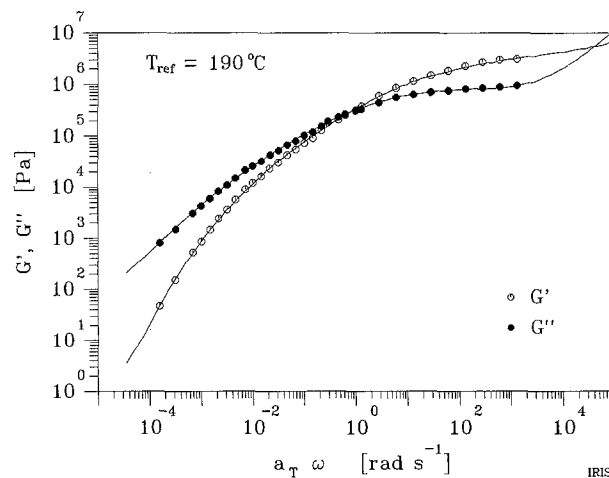

Fig. 6. Master curve of the storage and loss moduli, $G'(a_T\omega)$ and $G''(a_T\omega)$, respectively. The TRMS-generated master curve (symbols) was obtained by time-temperature superposition of the calculated $G'(\omega)$- and $G''(\omega)$-data. The lines represent a "normal" (from isothermal frequency sweeps) master curve measured by Baumgärtel (1990)

The frequency-dependent G'-, G''-data could be shifted onto a master curve with $T_{ref} = 190\,°C$ (Fig. 6). The TRMS-generated master curve agrees well with the "normal" (from isothermal frequency sweeps) master curve measured by Baumgärtel (1990). From this master curve the relaxation time spectrum (Fig. 7) was calculated which will be needed for the TRMS modeling calculations below.

The effect of heating rate is most pronounced at low frequencies (compare Fig. 8a and b). For our sample, G'-, G''-data at $\omega = 1$ rad/s (Fig. 8a) do not depend on the heating rate, even if the heating rate is high. Experiments at a lower frequency of $\omega = 0.1$ rad/s reach the acceptable limit at a heating rate of 5 K/min (see Fig. 8b). Below 5 K/min the results are independent of heating rate. However, G'-, G''-values are underestimated when the sample changes too fast. These observations clearly show the limits of the TRMS experiment.

Analysis and modeling of the TRMS experiment

The proposed method of data acquisition and analysis applies to experiments with sufficiently small mutation during the experimental time Δt. Values of N_{mu} or $N_{De}N_{mu}$ are a measure of the undergoing change. Critical mutation numbers for the studied system were obtained by using the rate of change of G' at the highest possible heating rate at which reliable data could be measured (boundary of quasi-stable region).
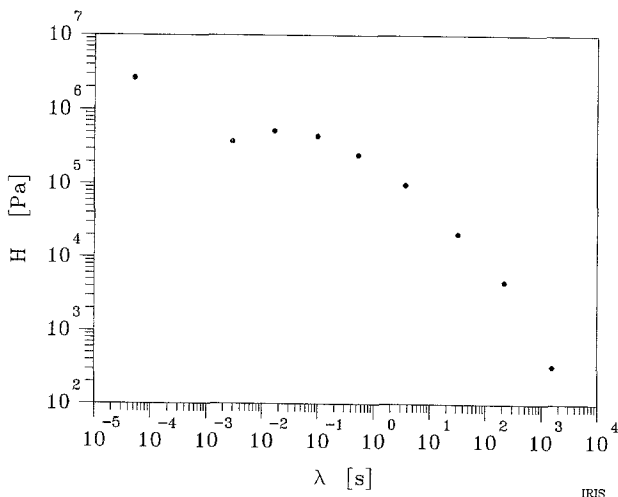

Fig. 7. Relaxation time spectrum $H(\lambda_i)$ of polycarbonate calculated by the standard program of Baumgärtel and Winter (1989)
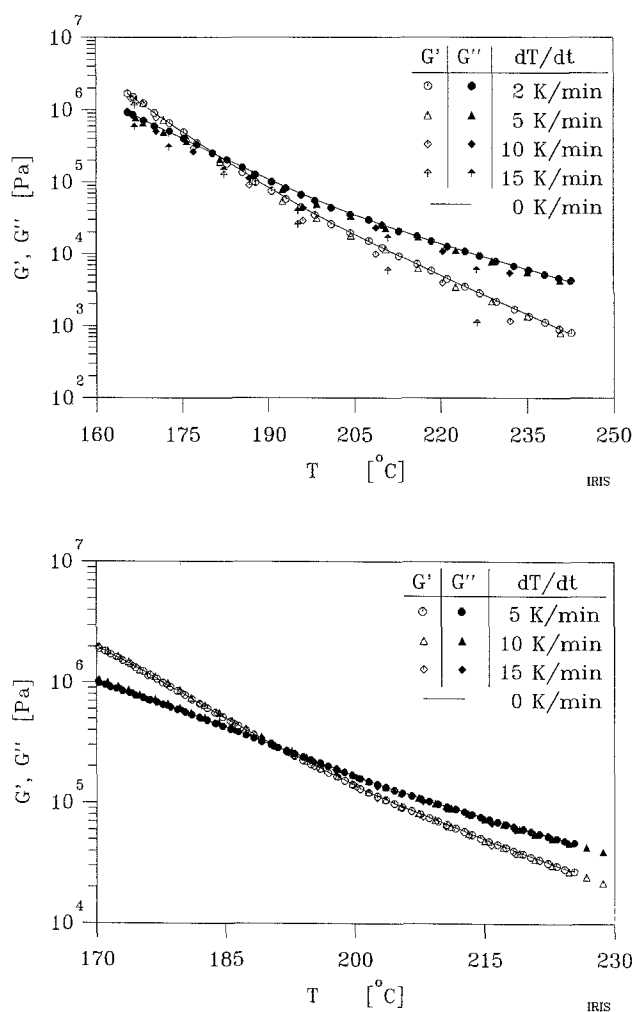

Fig. 8 a/b. Storage moduli $G'(t)$ and loss moduli $G''(t)$ of polycarbonate at several heating rates and two different frequencies (a (top) $\omega = 0.1$ rad/s and b (bottom) $\omega = 1$ rad/s). In the limiting case of 0 K/min the material was allowed to reach steady state at every probed temperature before the measurement was performed

Critical mutation numbers were calculated for different frequencies (i.e., different Δt) and different heating rates. The derivative $d\lg G'/dt$ was graphically obtained from plots of G' vs. time (Fig. 9).

Experimental times at probed frequencies were measured using a stopwatch. Experimental times Δt, critical heating rates, corresponding rates of change $\lambda_{mu}^{-1} = \dfrac{1}{G'}\dfrac{\partial G'}{\partial t} = \dfrac{\partial \ln G'}{\partial t}$, and calculated critical mutation numbers are listed in Table 1. Evidently, the data is still reasonable (i.e., in the quasi-stable region) up to $N_{mu} \cong 0.9$. Variations of $N_{mu,crit}$ (0.84 to 0.94) are within 7% and in the order of magnitude of the errors involved in the measurements and evaluation method.
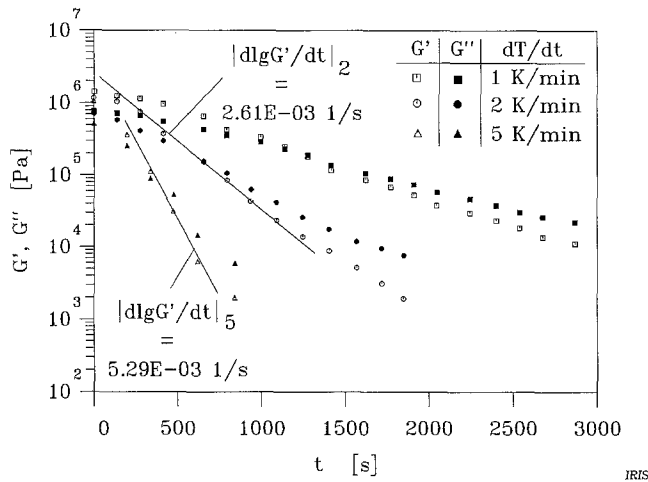
Fig. 9. Storage moduli $G'(t)$ and loss moduli $G''(t)$ of polycarbonate at different heating rates ($\omega = 0.05$ rad/s). The derivative $d\lg G'/dt$ can be obtained from this data

In order to determine the origins of TRMS limitation to mutation numbers smaller than 0.9 a computer simulation was performed to calculate the shear stress response as a function of time at increasing temperature and imposed oscillatory strain. The deviation of the stress from the sinusoidal form, which is still allowed for reasonable determination of G'-, G''-data, can be calculated subsequently.

The shear stress can be modeled by using Eqs. (2) and (15) and the discrete relaxation spectrum (g_i, λ_i) which was obtained from the experimental data (Eq. (16), Fig. 7):

$$\tau(t) = \int_{-\infty}^{t} \sum_{i=1}^{N} b_T(t) g_i \exp \left\{ -\frac{1}{\lambda_i} \int_{t'}^{t} \frac{dt''}{a_T(t'')} \right\} \dot{\gamma}_0$$

$$\cdot \cos(\omega t') dt' . \tag{18}$$

Table 1. Critical heating rates, experimental times Δt, derivatives $\partial \ln G'/\partial t$ and mutation numbers for different frequencies

Frequency [rad/s]	0.03	0.05	0.1	1
Δt [s]	340	150	110	9
Critical heating rate [K/min]	ca. 1	2	5	>15
$\partial \ln G'/\partial t$ [10^{-3} 1/s]	2.76	6	7.67	>16
$N_{mu,crit}$	0.94	0.9	0.84	>0.14

The integral can be split into two parts, one for the isothermal state for $-\infty < t' < 0$ and the second for the heating experiment where the temperature T is given by the linear profile of this experiment (for $t' > 0$ with $T_0 = 175\,°C$):

$$T(t') = T_0 + \frac{dT}{dt} t' . \tag{19}$$

Implementation of this equation in Eq. (18) results in the following expression for the shear stress τ:

$$\tau(t) = \sum_{i=1}^{N} \frac{b_{T_0} g_i \dot{\gamma}_0 a_{T_0} \lambda_i}{1 + (\omega a_{T_0} \lambda_i)^2} \exp\left(-\frac{t}{\lambda_i}\right) + \sum_{i=1}^{N} g_i \dot{\gamma}_0 \int_0^t b_T$$

$$\cdot \exp\left(-\frac{s(t,t')}{\lambda_i}\right) \cos(\omega t') dt' . \tag{20}$$

The isothermal part has an analytical solution while the contribution of the temperature scan requires a numerical approximation (Simpson-type numerical integration, Press et al., 1989).

The initial temperature of 175 °C corresponds to $a_{T_0} = 20$ when using a reference temperature of 190 °C. For times $t' > 0$ the same a_T-data (Table 2) can be used to evaluate the temperature-dependent shift factors. For small temperature intervals, a linear interpolation

$$a_T(T_{k-1} < T < T_k) = A_k + B_k T \tag{21}$$

is sufficiently accurate. The constants A_k and B_k for individual intervals as evaluated from the a_T-data are given in Table 2. This interpolation results in the reduced time $s(t, t')$ in Eq. (20) being equal to

$$s(t,t') = \frac{1}{dT/dt} \left(\frac{1}{B_{ki}} \ln\left(\frac{A_{ki} + B_{ki} T_{ki}}{A_{ki} + B_{ki} T(t')}\right) \right.$$

$$+ \sum_{k = ki+1}^{kf} \frac{1}{B_k} \ln\left(\frac{A_k + B_k T_k}{A_k + B_k T_{k-1}}\right)$$

$$\left. + \frac{1}{B_{kf+1}} \ln\left(\frac{A_{kf+1} + B_{kf+1} T(t)}{A_{kf+1} + B_{kf+1} T_{kf}}\right) \right) , \tag{22}$$

where k_i denotes the index of the next T_k higher than $T(t')$ and k_f denotes the index of the next T_k lower than $T(t)$ (see Table 2).

The vertical shift factors, b_T, of PC Lot 150 are close to unity (see Table 2) which means that the ver-
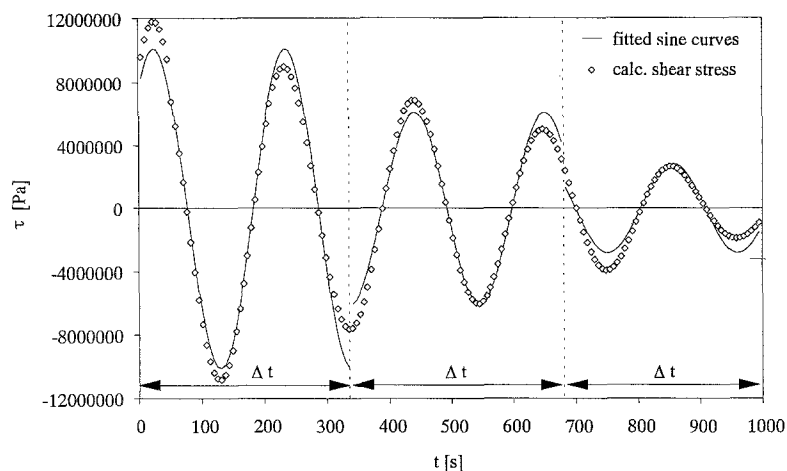
Fig. 10. Calculated shear stress and fitted sine curves for $\omega = 0.03$ rad/s and a heating rate of 1 K/min. Sine curves (constant amplitude) were fitted by least-square approximation to obtain values for τ_0 and δ as needed in Eqs. (8) and (9) for calculation of G' and G''. This must be repeated for every consecutive experimental time interval Δt to yield time-dependent G'-, G''-data. In this case ($\omega = 0.03$ rad/s) the experimental time Δt was 340 s (see Table 2). Three time intervals yielding three data points (for each G' and G'') are shown here

tical shift can be neglected in most parts of the simulation.

In order to compare the calculated shear stress response with experimental data (G', G'') it was necessary to extract G'- and G''-data directly from the shear stress simulation. This was done as follows: Sine curves [$\tau = \tau_0 \sin(\omega t + \delta)$] were fitted to the simulated $\tau(t)$ for each experimental time period Δt (time required by the rheometer for a single measurement as given in Table 1) (Fig. 10). For each data point (G' and G''), the time at the beginning of the measurement (experimental time period) was assigned as time at which this data point was taken, since it seems that the rheometer control software also assigns an early time. For the example in Fig. 10, the deviation between local sine-fit and the evolving $\tau(t)$ is rather large since N_{mu} is relatively large here.

These approximations yielded mean values (for each time interval Δt) for the shear stress amplitude

τ_0 and the loss angle δ which are necessary to evaluate G' and G'' for each Δt (see Eqs. (8) and (9)).

Figure 11 shows such calculated G'-, G''-data ($\omega = 0.1$ rad/s, different heating rates) in comparison to measured values ($\omega = 0.1$ rad/s, 2 K/min). The calculated data at heating rates of 1 and 2 K/min are almost identical and show good agreement with the measured moduli. In these cases, the differences between calculated and fitted $\tau(t)$ (as in Fig. 10) and hence the property changes during one measurement are rather small. The material behaves quasi-stable and the measurement results in reliable data. At higher heating rates, the values for the moduli decrease significantly.

Table 2. Vertical and horizontal shift factors (b_T and a_T, respectively) for PC Lot 150 and parameters A_k and B_k (Eq. (21))

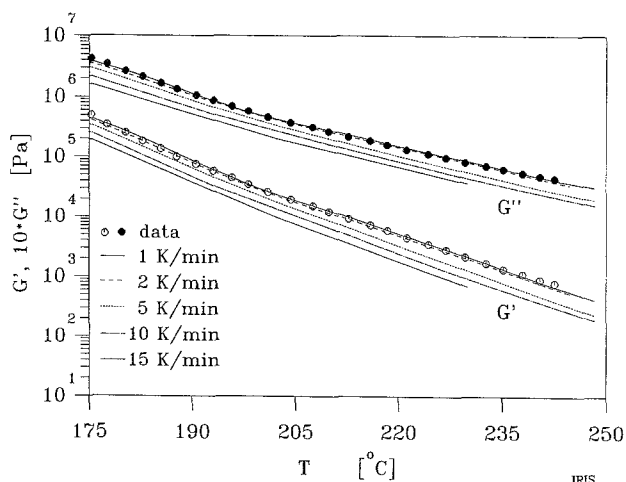| T_k [°C]	b_T	a_T	A_k	B_k [1/K]
175	1.04	$2.00 \cdot 10^1$		
180	1.07	$8.71 \cdot 10^0$	$4.13 \cdot 10^2$	$-2.25 \cdot 10^0$
190	1.00	$1.00 \cdot 10^0$	$1.47 \cdot 10^2$	$-7.71 \cdot 10^{-1}$
200	1.02	$2.04 \cdot 10^{-1}$	$1.61 \cdot 10^1$	$-7.96 \cdot 10^{-2}$
220	0.91	$3.16 \cdot 10^{-2}$	$1.93 \cdot 10^0$	$-8.63 \cdot 10^{-3}$
240	0.83	$7.41 \cdot 10^{-3}$	$2.98 \cdot 10^{-1}$	$-1.21 \cdot 10^{-3}$
260	0.78	$2.34 \cdot 10^{-3}$	$6.82 \cdot 10^{-2}$	$-2.53 \cdot 10^{-3}$
275	0.72	$1.15 \cdot 10^{-3}$	$2.31 \cdot 10^{-2}$	$-7.97 \cdot 10^{-4}$

Fig. 11. Measured storage and loss moduli, $G'(t)$ and $G''(t)$ respectively, at $\omega = 0.1$ rad/s and a heating rate of 2 K/min (symbols) plus calculated $G'(t)$ and $G''(t)$ for different heating rates

Discussion

Time-resolved rheometry allows probing of a whole class of transient materials such as polymers during gelation, phase transition, decomposition, polymerization, etc., as long as the structural changes occur sufficiently slow. If the changes during the experimental time Δt are sufficiently small (i.e., small N_{mu} or $N_{De}N_{mu}$), correct values of the moduli, Eqs. (8) and (9), can still be evaluated since the shear stress response is still nearly sinusoidal during Δt, i.e., the amplitude and the phase angle do not change substantially. However, if the total property change during the experimental time exceeds a critical value, the shear stress response is no longer nearly sinusoidal (Fig. 10) and measured values of G' and G'' deviate from the data on stable samples. One goal of the present study was to estimate the boundary of the region of quasi-stable response.

The experimental data at different heating rates (Fig. 8a, b) show deviations from the quasi-stable behavior at low frequencies and high heating rates. Thermal inertia might cause the temperature within the sample to be non-uniform and lower than the indicated temperature. Surprisingly, the data at a frequency of 1 rad/s coincide for all heating rates. This indicates that the sample temperature must be at least close to the measured temperature (= temperature of the bottom plate in the rheometer). A certain compensation effect might occur (higher heating rates result in an apparent decrease of measured G' and G'' while a lower sample temperature would give rise to higher values of the moduli). However, a detailed study of these phenomena was not intended here. If necessary, additional experiments with a thermocouple embedded in the sample might be advisable.

Using the non-isothermal model it was possible to calculate shear stress, τ, and dynamic moduli, G', G'', at different frequencies and heating rates. Figure 11 compares measured and calculated G'-, G''-data for a given frequency and heating rates and calculated data for several heating rates. Reasonable agreement between measured and calculated data is readily seen. The calculated curves reveal that at low heating rates (1 and 2 K/min) the data is essentially independent of heating rate. A significant decrease can be seen at higher heating rates (≥ 5 K/min) which is also in good agreement with the experiments (Fig. 8b). This drop results from the averaging effect of the measurement over the entire experimental time period. The shear stress data of the entire period Δt is used to calculate amplitude and phase angle. At the end of this period the material is already at a much higher temperature

and the shear stress response is therefore much lower than for the lower temperature at the beginning. Hence, the average value is lower than the real value at the given temperature. No thermal inertia effects are included in these modeled data. The sensitivity of the experiment to the heating rate however depends on the time assigned to each data point. If an intermediate time rather than an early time of the time interval Δt is chosen, the averaged G'-, G''-data might coincide with the "real" value at this particular time (temperature).

The maximum relative change of the shear stress amplitude τ_0 (Fig. 12) and the loss angle δ during the experimental time Δt (for every frequency and heating rate) was taken from the sinusoidal shear stress response. At the experimentally determined critical heating rates (s. Table 1) relative changes of τ_0 of about 90% can be found.

Changes of the loss angle δ during Δt increase almost linearly with heating rate, but are small compared to changes of τ_0 (only about 10% at the critical heating rates). Therefore, influences of the change of δ on the mutation number can approximately be neglected. In this case the mutation number can be expressed as

$$N_{mu} = \Delta t \frac{1}{G'} \frac{\partial G'}{\partial t} \cong \Delta t \frac{1}{\tau_0} \frac{\partial \tau_0}{\partial t} \cong \frac{\Delta \tau_0}{\tau_0} . \qquad (23)$$

This results in a calculated value for $N_{mu,crit}$ of 0.9 which is the same as the experimentally determined one.

The differences between the experimental G'-, G''-data at low and high heating rates (quasi-stable and non-stable region, respectively) are fairly small (max. 10%) in spite of a very high mutation number.
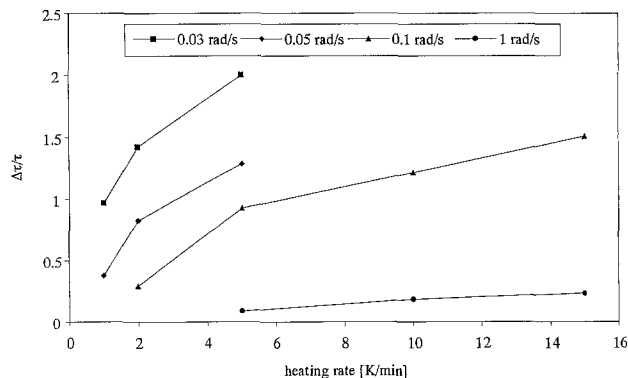

Fig. 12. Maximum relative changes of the shear stress amplitude τ_0 during one measurement (experimental time Δt) for all frequencies and heating rates

Chambon et al. (1986) and Winter et al. (1988) concluded from their gelation data that non-linear behavior can be observed at mutation numbers higher than 0.15. Since the critical mutation numbers found in this study mainly reflect the change of the shear stress amplitude τ_0, influences of rapid changes of the loss angle δ cannot be accounted for. Such rapid changes might occur during other types of mutation and could result in lower critical mutation numbers.

One of the most rewarding aspects of the study is the agreement between the experiment and the modeling. Time-temperature superposition of the polycarbonate data makes the modeling possible and much insight was gained from it. The time shift in the rheological behavior was simply described by a temperature-dependent function while the shape of $H(\lambda)$ remained constant (Eq. (16)). This makes it clear that we could not yet provide a complete answer to the problem, especially with our interest in changing material structure which causes changes in both, $H(\lambda)$ and a_T. Mutation is a much more complicated situation than time-temperature shifting during heating and we currently have no means of formulating a complete model of the TRMS experiment. For the time being, we characterize mutating materials with TRMS and assume that, in spite of the materials' complex structural changes, TRMS is still applicable. The most recent TRMS study on crosslinking polybutadienes (DeRosa et al., 1994) gave self consistent results in support of this assumption. A constitutive equation for the crosslinking material would be required to include mutation in the future modeling of the TRMS experiment.

Conclusions

Time-resolved mechanical spectroscopy (cyclic frequency sweeps in combination with a computerized data treatment) can be applied to determine frequency-dependent data and relaxation time spectra at intermediate states of transient materials. In previous studies, TRMS was successfully applied to characterize gelation processes (Scanlan et al., 1991). However, a detailed analysis of its applicability and limits was never performed. In this study, non-isothermal changes were investigated as a paradigm for a mutating sample. It was shown that TRMS can be employed if the sample behaves quasi-stable during all experimental times Δt. This was quantified by means of a critical mutation number $N_{mu,crit}$ [N_{mu} = (experimental time)/(mutation time) = experimental time·rate of change]. A constant value of 0.9 for

$N_{mu,crit}$ was found experimentally. Therefore, the possible rate of change decreases with decreasing frequency (Eq. 13a,b).

Simulations of the shear stress response to an imposed oscillatory strain were performed. Values for G' and G'' were extracted and compared to experimental data. Reasonable agreement was found, proving that the shear stress behavior in non-isothermal small amplitude oscillatory shear experiments is well described by the model of Hopkins, and Morland and Lee (Eq. (15)). A distinct decrease in the calculated moduli was found for heating rates larger than a certain critical heating rate, resulting in a frequency-independent critical mutation number. Below this critical heating rate, the calculated moduli are nearly independent of the heating rate. This critical mutation number was found to be closely related to the maximum relative change of the shear stress amplitude $(\Delta \tau_0/\tau_0)$ during the experimental time Δt. An influence of the rate of change of the loss angle δ on the mutation number could not be detected since the change of δ during the individual experimental times Δt was small.

The critical mutation number of non-isothermal relaxation cannot necessarily be transferred to other transient phenomena such as gelation or phase separation because the rate of mutation might have a stronger influence on δ for these cases. Different limitations to TRMS might then exist (lower $N_{mu,crit}$). Reasons for such limitations could only be investigated if a satisfying model for the functional $\underset{t''=t'}{\overset{t''=t}{G}} (t,t',p(t''))$ existed. Therefore, future studies should concentrate on the determination of a constitutive equation (resulting in $\underset{t''=t'}{\overset{t''=t}{G}} (t,t',p(t''))$ for crosslinking polymers, polymers during phase separation, etc. This would also lead to an interrelation between stable and non-stable response which could be used to extend application of time-resolved mechanical spectroscopy to the non-stable region.

Appendix

It is a well accepted assumption that mechanical spectroscopy predominantly probes the relaxation modes with relaxation time values near $\lambda = 1/\omega$, where ω is the frequency used in the dynamic mechanical measurement. To examine this assumption we use an arbitrary power law spectrum:

$$H = H_1 \left(\frac{\lambda}{\lambda_1}\right)^{-n} . \tag{24}$$

The ends of the power law region are unimportant here since we are interested in the behavior near a reference point on the spectrum (H_1, λ_1). The storage and loss moduli are then specified by (Ferry, 1980)

$$G'(\omega) = \int_{-\infty}^{+\infty} H(\lambda) \frac{(\omega\lambda)^2}{1 + (\omega\lambda)^2} \, d\lg \lambda$$

$$= H_1 \int_{-\infty}^{+\infty} \left(\frac{\lambda}{\lambda_1}\right)^{-n} \frac{(\omega\lambda)^2}{1 + (\omega\lambda)^2} \, d\lg \lambda \tag{25}$$

$$G''(\omega) = \int_{-\infty}^{+\infty} H(\lambda) \frac{\omega\lambda}{1 + (\omega\lambda)^2} \, d\lg \lambda$$

$$= H_1 \int_{-\infty}^{+\infty} \left(\frac{\lambda}{\lambda_1}\right)^{-n} \frac{\omega\lambda}{1 + (\omega\lambda)^2} \, d\lg \lambda . \tag{26}$$

The question which we would like to answer is the following: Which part of the spectrum determines G' and G'' if we probe the above material (represented by Eq. (24)) at a frequency $\omega = 1/\lambda_1$? Substituting $\omega\lambda$ with $\lambda/\lambda_1 = x$ results in

$$G'(\omega = 1/\lambda_1) = H_1 \int_{-\infty}^{+\infty} x^{-n} \frac{x^2}{1 + x^2} \, d\ln x$$

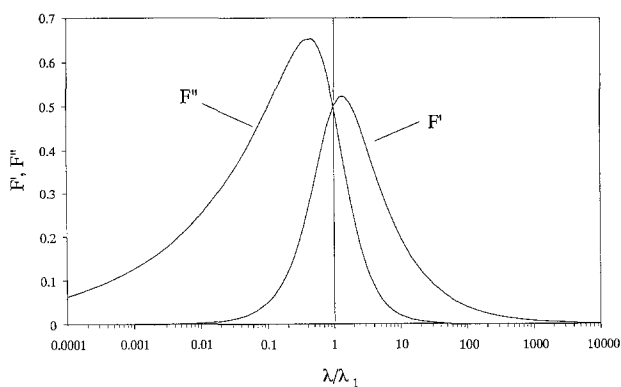$$= H_1 \int_{-\infty}^{+\infty} F' \, d\ln x \tag{27}$$

Fig. 13. Integral kernels of Eqs. (27) and (28), $F'(\lambda/\lambda_1)$ and $F''(\lambda/\lambda_1)$, for the evaluation of $G'(\omega = 1/\lambda_1)$ and $G''(\omega = 1/\lambda_1)$, respectively

$$G''(\omega = 1/\lambda_1) = H_1 \int_{-\infty}^{+\infty} x^{-n} \frac{x}{1 + x^2} \, d\ln x$$

$$= H_1 \int_{-\infty}^{+\infty} F'' \, d\ln x . \tag{28}$$

Figure 13 shows plots of F' and F'' as a function of λ/λ_1 using a typical value for n ($n = 0.7$). The dynamic moduli are simply the areas under the curves multiplied by a constant factor H_1. It can be seen that the dominating contribution results from relaxation times close to $\lambda = \lambda_1 = 1/\omega$.

References

Baumgärtel M, Winter HH (1989) Determination of discrete relaxation and retardation time spectra from dynamic mechanical data. Rheol Acta 28:511 – 519
Baumgärtel M (1990) unpublished results
Bird RB, Armstrong RC, Hassager O (1987) Dynamics of polymeric liquids, 2. ed. J Wiley & Sons, New York
deBoor C (1978) A practical guide to splines. Appl Math Sci, Vol 27, Springer-Verlag, Berlin
Chambon F, Winter HH (1985) Stopping of crosslinking reaction in a PDMS polymer at the gel point. Polym Bull 13:499 – 503
Chambon F, Petrovic ZS, MacKnight WJ, Winter HH (1986) Rheology on model polyurethanes at the gel point. Macromol 19:2146 – 2149
Craven P, Wahba G (1979) Smoothing noisy data with spline functions. Num Math 31:377 – 403
DeRosa ME, Winter HH (1994) The effect of entanglements on the rheological behavior of polybutadiene critical gels. Rheol Acta 33 (in press)
Ferry J (1980) Viscoelastic properties of polymers, 3. ed. J. Wiley & Sons, New York
Holly EE, Venkataraman SK, Chambon F, Winter HH (1988) Fourier transform mechanical spectroscopy of viscoelastic materials with transient structure. J Non-Newtonian Fluid Mech 27:17 – 26
Hopkins IL (1958) Stress relaxation or creep of linear viscoelastic substances under varying temperature. J Pol Sci 28:631 – 633
Morland LW, Lee EH (1960) Stress analysis for linear viscoelastic materials with temperature variation. Trans Soc Rheol 4:233 – 263
Press WH, Flannery BP, Teukolsky SA, Vetterling WT

(1989) Numerical recipes, the art of scientific computation. Cambridge University Press, Cambridge

Reiner M (1964) The Deborah number. Physics Today 17:62

Reinsch C (1967) Smoothing by spline functions. Num Math 10:177 – 183

Scanlan JC, Winter HH (1991) The evolution of viscoelasticity near the gel point of endlinking poly(dimethylsiloxane)s. Makromol Chem, Macromol Symp 45: 11 – 21

Scanlan JC, Winter HH (1991) Composition dependence of the viscoelasticity of end-linked poly(dimethylsiloxane). Macromol 24:47 – 54

Wahba G (1990) Spline models for observational data. Society for Industrial and Applied Mathematics, Philadelphia

Winter HH, Chambon F (1986) Analysis of linear viscoelasticity of a crosslinking polymer at the gel point. J Rheol 30:367 – 382

Winter HH, Morganelli P, Chambon F (1988) Stoichiometry effects on rheology of model polyurethanes at the gel point. Macromolecules 21:532 – 535

Correspondence to:

Prof. H. Henning Winter
Dept. of Chemical Engineering
University of Massachusetts
Amherst, MA 01003
USA